Ángel F. Doval and Cristina Trillo, "Hybrid optonumerical quasi Fourier transform digital holographic camera," Proc. SPIE 6341, "Speckle06: Speckles, From Grains to Flowers," 63410Z (September 15, 2006)

http://dx.doi.org/10.1117/12.695340

Hybrid optonumerical quasi Fourier transform digital holographic camera

Ángel F. Doval* and Cristina Trillo

Universidad de Vigo. Departamento de Física Aplicada.
E.T.S. de Ingenieros Industriales. Campus Universitario. E36310 Vigo (Spain). *adoval@uvigo.es

ABSTRACT

We present a novel hybrid digital holographic camera which shares most of the advantages of image-plane Fourier transform TV holography (TVH) and quasi-Fourier transform digital holography (QFTDH), whilst avoiding many of the drawbacks of both of them. As in TVH, it has a compact head where an objective lens is attached to accommodate objects of different sizes or placed at different distances; it is also free from aliasing artifacts produced by objects out of the field of view. As in QFTDH, the reconstruction of the object field (amplitude and phase) is accomplished by calculating just one fast Fourier transform (FFT) per hologram; light is spread over the sensor rather than being focused to produce an image, thus enabling the measurement in objects with very large radiance ranges.

An optical imaging system (typically a zoom lens) selects the field of view and the working distance by projecting a reduced image of the object on the plane of a rectangular aperture. This image becomes the object for a lensless quasi-Fourier transform digital hologram, which is formed by making the light passing through the aperture to interfere with a reference beam diverging from its edge. This hologram is recorded with a video camera, digitized and numerically reconstructed by means of a single FFT. The function of the aperture is to crop the field of view to make the effective object size suitable to be recorded without aliasing on a sensor with a given pixel spacing; therefore, its size is determined by this spacing, the distance between the aperture and the sensor as well as by the wavelength of light.

Keywords: Fourier transform digital holography, TV holography

1. INTRODUCTION

Fourier transform TV holography[1] (TVH) is a well established measurement technique which is specially useful for the measurement of transient events, where all the information has to be gathered by recording just one or two interferograms. Nevertheless, is has some aspects whose improvement would be valuable for certain applications. On the one hand, in TVH an image of the object to be measured is projected on the sensor of a video camera and when the object is a bad diffuser and presents specular reflections on its surface, these areas often appear saturated in the recorded interferogram and cannot be measured. On the other hand, the Fourier transform phase evaluation method generally applied in TV holography uses two full field numerical Fourier transforms, which are time-consuming calculations even if a fast Fourier transform (FFT) algorithm is used. Eliminating one of the two FFTs would save a relevant amount of time whenever a very large number of measurements has to be made.

Digital holography[2] can be an alternative to TVH in such circumstances, particularly lensless quasi Fourier-transform digital holography[3] (QFTDH). In this family of techniques the hologram is recorded without forming an image of the object and, therefore, they are reasonably tolerant to specular reflections; furthermore, the basic reconstruction of the hologram is accomplished with a single FFT. But QFTDH lacks the flexibility of TVH to make remote measurements because the reference beam has to diverge from a point near the object and the distance between the object and the hologram has to be set according to the resolution limits of the camera and to the size of the object. Objects which are too large, too close or out of the theoretical field of view usually produce undesirable aliasing effects.

An hybrid technique using a lens to select the field of view and the main focusing position by projecting a reduced image of the object at a fixed position near the video camera, and recording a digital lensless Fourier-transform hologram of this image, rather than of the object, would share most of the advantages of TVH and QFTDH.

The idea of combining image formation optics with lensless Fourier-transform holography has been recently put into practice in the field of holographic microscopy[4]. Following this principle, we propose the design of a compact hybrid digital holographic camera, capable of making holographic interferometric measurements, which can be coupled to practically any image-forming optical system such as a photographic objective, a microscope, a telescope, an endoscope, etc.

Speckle06: Speckles, From Grains to Flowers, edited by Pierre Slangen, Christine Cerruti,
Proc. of SPIE Vol. 6341, 63410Z, (2006) · 0277-786X/06/$15 · doi: 10.1117/12.695340

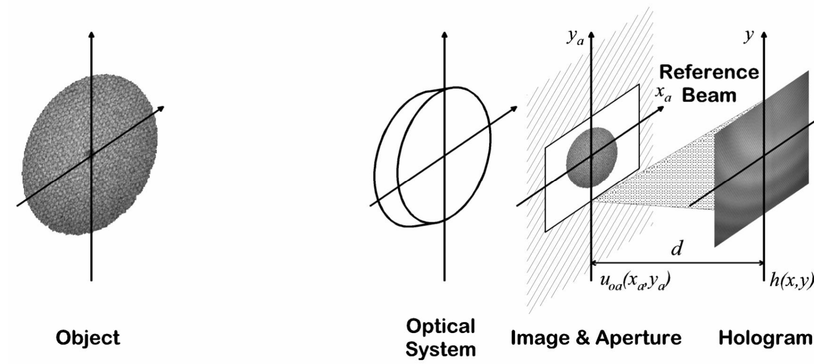

Figure 1. Optical scheme for the formation of a lensless Fourier-transform hologram from an image projected on the plane of the reference beam source, where a field-limiting aperture is placed.

2. THEORY

2.1. Formation and reconstruction of a quasi-Fourier transform hologram of the image of an optical system

Given that $u_{oa}(x_a , y_a)$ is the object beam at the plane of the image of the object projected by an optical system, where an aperture has been placed to limit its size, and that a reference beam $u_{ra}(x_a , y_a) = A_r\, \delta(x_a - x_{ar} , y_a - y_{ar})$ is made to diverge from a point (x_{ar} , y_{ar}) of the same plane, as shown in figure 1, it is well known[5] that after propagating in free space and interfering at a plane placed at a given distance d from the aperture they yield an irradiance distribution which, once recorded, forms a kind of quasi-Fourier transform hologram called a lensless Fourier-transform hologram:

$$h(x,y) = \left|u_{oh}(x,y)\right|^2 + \frac{A_r^{\,2}}{d^2} + A_r C \hat{U}_{oa}\left(\frac{x}{\lambda d},\frac{y}{\lambda d}\right)\exp\left[-j\frac{2\pi}{\lambda d}(x\,x_{ar} + y\,y_{ar})\right] + A_r C^* \hat{U}^*_{oa}\left(\frac{x}{\lambda d},\frac{y}{\lambda d}\right)\exp\left[j\frac{2\pi}{\lambda d}(x\,x_{ar} + y\,y_{ar})\right] \quad (1)$$

with

$$\hat{U}_{oa}(x,y) = \mathfrak{F}\left\{\exp\left[j\frac{\pi}{\lambda d}(x_a^{\,2} + y_a^{\,2})\right] \; u_{oa}(x_a, y_a)\right\} \quad (2)$$

where (x , y) are the coordinates of the hologram plane, λ is the wavelength of light, C is complex constant and $\mathfrak{F}$ stands for the Fourier transform.

The reconstruction of this type of holograms can be accomplished by either the direct or the inverse Fourier transform. Let us take, for convenience, the direct transform of equation (1):

$$H(f_x , f_y) = \mathfrak{F}\,[h(x , y)] = H_o(f_x , f_y) + H_r(f_x , f_y) + H_{or}^{\;+}(f_x , f_y) + H_{or}^{\;-}(f_x , f_y) \quad (3)$$

The first two terms

$$H_o(f_x, f_y) = \mathfrak{F}\{|u_{oh}(x,y)|^2\} = U_{oh}(f_x, f_y) * U^*_{oh}(-f_x, -f_y) = u_{oa}(-\lambda d f_x, -\lambda d f_y) * u^*_{oa}(\lambda d f_x, \lambda d f_y) \quad (4)$$

$$H_r(f_x , f_y) = \mathfrak{F}\left\{\frac{A_r^{\,2}}{d^2}\right\} = \frac{A_r^{\,2}}{d^2}\,\delta(f_x , f_y) \quad (5)$$

are, respectively, a scaled image of the complex autocorrelation of the object beam at the aperture plane which appears as a diffuse halo and an image of the reference beam, also at the aperture plane, which appears as a bright spot, both images are centered in the frequency space. The remaining two terms, called the interferometric terms:

$$H_{or}^{\;+}(f_x, f_y) = \mathfrak{F}\left\{A_r C \hat{U}_{oa}\left(\frac{x}{\lambda d},\frac{y}{\lambda d}\right)\exp\left[-j\frac{2\pi}{\lambda d}(x\,x_{ar} + y\,y_{ar})\right]\right\} \quad (6)$$

$$H_{or}^{\;-}(f_x, f_y) = \mathfrak{F}\left\{A_r C^* \hat{U}^*_{oa}\left(\frac{x}{\lambda d},\frac{y}{\lambda d}\right)\exp\left[j\frac{2\pi}{\lambda d}(x\,x_{ar} + y\,y_{ar})\right]\right\} \quad (7)$$

are symmetrically shifted respect to the center of the frequency plane and somehow related to the object beam. Let us consider the first one

$$H_{\mathrm{or}}^{+}(f_x,f_y)=A_{\mathrm{r}}C\,\mathfrak{F}\{\hat{U}_{\mathrm{oa}}(x,y)\exp[-j2\pi(x\,x_{\mathrm{ar}}+y\,y_{\mathrm{ar}})]\}_{(\lambda df_x,\lambda df_y)}=A_{\mathrm{r}}C\,\mathfrak{F}\{\hat{U}_{\mathrm{oa}}(x,y)\}_{(\lambda df_x+x_{\mathrm{ar}},\lambda df_y+y_{\mathrm{ar}})} \quad (8)$$

by substituting equation (2) results

$$\begin{aligned}H_{\mathrm{or}}^{+}(f_x,f_y)&=\lambda^2d^2A_{\mathrm{r}}C\,\mathfrak{F}\left\{\mathfrak{F}\left\{\exp\left[j\frac{\pi}{\lambda d}(x^2+y^2)\right]\;u_{\mathrm{oa}}(x,y)\right\}\right\}_{(\lambda df_x+x_{\mathrm{ar}},\lambda df_y+y_{\mathrm{ar}})}\\&=\lambda^2d^2A_{\mathrm{r}}C\exp\left\{j\frac{\pi}{\lambda d}[(\lambda df_x+x_{\mathrm{ar}})^2+(\lambda df_y+y_{\mathrm{ar}})^2]\right\}\;u_{\mathrm{oa}}\left[-(\lambda df_x+x_{\mathrm{ar}}),-(\lambda df_y+y_{\mathrm{ar}})\right]\end{aligned} \quad (9)$$

which, except for an object-independent phase factor —which, if necessary, can be easily calculated and removed—, is an scaled and shifted image of the object beam at the aperture plane, where

$$f_x=-\frac{x_{\mathrm{a}}+x_{\mathrm{ar}}}{\lambda d}\quad;\quad f_y=-\frac{y_{\mathrm{a}}+y_{\mathrm{ar}}}{\lambda d} \quad (10)$$

2.2. Numerical reconstruction of the digitally sampled hologram

In our case, the hologram is recorded by a camera, spatially sampled according to its pixel spacing ($\Delta x\times\Delta y$) and digitized into an $M\times N$ array of pixels. The values of the elements in this array are

$$h(m\,,n)=h(m\,\Delta x,n\,\Delta y)\quad;\quad 0\le m<M\quad,\quad 0\le \mathrm{n}<N \quad (11)$$

Since the object-independent phase factor is usually irrelevant for most of applications, the numerical reconstruction process is implemented by means of a single fast Fourier transform (FFT). Though not strictly necessary, it is usual to swap the quadrants of the resulting array to render an optical representation of the transform with the origin at the center

$$H(p,q)=H(p\Delta f_x,q\Delta f_y)=\mathrm{FFT}[h(m,n)]\quad;\quad -\left(\frac{M}{2}-1\right)\le p\le\frac{M}{2}\quad,\quad -\left(\frac{N}{2}-1\right)\le q\le\frac{N}{2} \quad (12)$$

The frequency spacing ($\Delta f_x\times\Delta f_y$) is related to the size ($X\times Y$) of the hologram, as follows

$$\Delta f_x=\frac{1}{M\Delta x}=\frac{1}{X}\quad;\quad \Delta f_y=\frac{1}{N\Delta y}=\frac{1}{Y} \quad (13)$$

what, together with equation (10), gives the correspondence between the pixels of the reconstruction of the object beam $H_{\mathrm{or}}^{+}(p\,,q)$ and the position on the aperture plane $u_{\mathrm{oa}}(x_{\mathrm{a}}\,,y_{\mathrm{a}})$

$$x_{\mathrm{a}}=-\left(x_{\mathrm{ar}}+p\frac{\lambda d}{M\Delta x}\right)\quad;\quad y_{\mathrm{a}}=-\left(y_{\mathrm{ar}}+q\frac{\lambda d}{N\Delta y}\right) \quad (14)$$

2.3. Application to holographic interferometry

The modulus of the reconstruction of the hologram $|H(p\,,q)|$ shows the two symmetrical reconstructions of the focused image projected by the optical system on the aperture plane. When temporal treatment techniques like time averaging or double pulse stroboscopic illumination, which produce an amplitude modulation[6] of the hologram, are applied the resulting interferometric fringes will appear in this modulus.

On the other hand, the phase of the reconstruction can be calculated to implement interferometric techniques based on the modulation of the phase of the hologram. The phase of the reconstructed holograms generally has a random distribution and useful information is obtained from its change between two exposures h_1 and h_2. Rather than subtracting the arguments of the two reconstructions H_1 and H_2, what would result in a number of randomly distributed phase jumps, it is preferable to calculate the phase difference as[7]

$$\Delta\Phi=\arg(H_2\;H_1^{*}) \quad (15)$$

2.4. Separation of the interferometric terms

The four terms of equation (3) are simultaneously reconstructed and appear, in general, superimposed. This is not a severe handicap when working on a phase-difference basis, as stated above, since the non-interferometric terms are cancelled in the subtraction process. It has just to be ensured that the two symmetrical interferometric terms are neither overlapped nor aliased. It can be easily derived from equation (14) that the maximum dimensions ($X_{\mathrm{a}}\times Y_{\mathrm{a}}$) of the aperture which satisfy this condition and, therefore, maximize the use of the resolution of the camera are

$$X_a = \frac{\lambda d}{\Delta x} \quad , \quad Y_a = \frac{\lambda d}{2\Delta y}$$ with the reference beam diverging from the center of one of the X sides. (16)

or $$X_a = \frac{\lambda d}{2\Delta x} \quad , \quad Y_a = \frac{\lambda d}{\Delta y}$$ with the reference beam diverging from the center of one of the Y sides. (17)

For a camera with "square" pixels ($\Delta x = \Delta y$) this means a rectangular aperture with 2:1 aspect ratio.
When working on an amplitude basis the non-interferometric terms become apparent, particularly the autocorrelation of the object beam, equation (4), which spreads over an equivalent area of $2X_a \times 2Y_a$ centered on the image of the reference beam and can overlap and mask the reconstructions of the image of the object. Two object-independent approaches can be taken to overcome this problem: spectrum and amplitude separation.
To completely separate the frequency spectra of the autocorrelation of the object beam and of the reconstructed image, it follows from equation (14) that the size of the aperture has to be reduced to a maximum of

$$X_a = \frac{\lambda d}{\Delta x} \quad , \quad Y_a = \frac{\lambda d}{4\Delta y}$$ with the reference beam Y_a away from the center of one of the X sides. (18)

or $$X_a = \frac{\lambda d}{4\Delta x} \quad , \quad Y_a = \frac{\lambda d}{\Delta y}$$ with the reference beam X_a away from the center of one of the Y sides. (19)

For a camera with "square" pixels ($\Delta x = \Delta y$) this means a rectangular aperture with an unpleasant 4:1 aspect ratio.
Amplitude separation is a less rigorous method but allows to keep the size of the aperture as stated in equations (16) and (17). It consists in increasing the intensity of the reference beam until, for regular objects, the amplitude of the autocorrelation of the object beam, equation (4), which does not depend on the reference beam, can be neglected against the interferometric terms, equations (6) and (7), which are proportional to the amplitude of the reference beam.
The image of the reference beam is less problematic. Though extremely intense, it is highly localized around the center of the frequency space and, furthermore, since it is object-independent and with the proposed design its position respect to the sensor is fixed, its amplitude can be recorded and reconstructed once without the presence of the object beam and subsequently subtracted from the amplitude of the following reconstructions.

3. EXPERIMENT AND RESULTS

We have implemented the proposed technique by assembling a digital holographic camera as shown in figure 2. The compact head comprises a digital monochrome camera with a 1/2" (6,5mm×4,8mm) sensor and a pixel spacing $\Delta x = \Delta y = 4{,}65\mu m$ (1392×1040 pixels), a rectangular aperture with the same size than the sensor and fixed to the camera at a distance $d = 2\Delta y Y_a / \lambda \approx 70mm$ according to equation (16), and a conectorized optical fiber which delivers the reference beam to the center of the long side of the aperture. The frontmost element is the elbow of the reference beam fiber which protrudes about 5mm from the aperture plane, this allows to use either photographic or C-mount interchangeable objectives (17,5mm back clearance) to form the image of the object on the aperture plane. The diaphragm of the objective must be fully open since the aperture in front of the camera plays the roles of both field and aperture stop.
The object and reference beams are delivered through optical fibers. A polarization controller and an adjustable attenuator in the reference beam allow, respectively, to match the polarization of the beams to maximize interference and to perform the amplitude separation of the reconstructed images as specified in section 2.4.

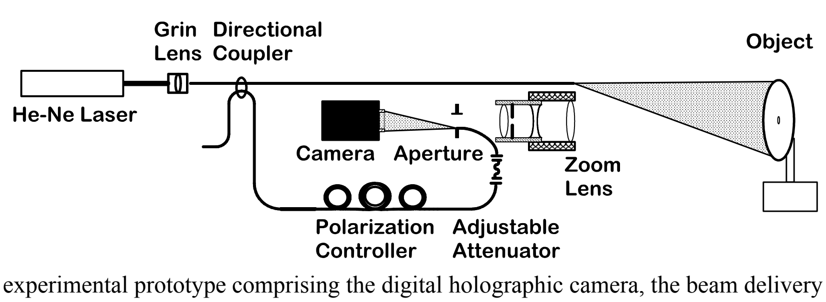

Figure 2. Layout of the experimental prototype comprising the digital holographic camera, the beam delivery fibers and the object.

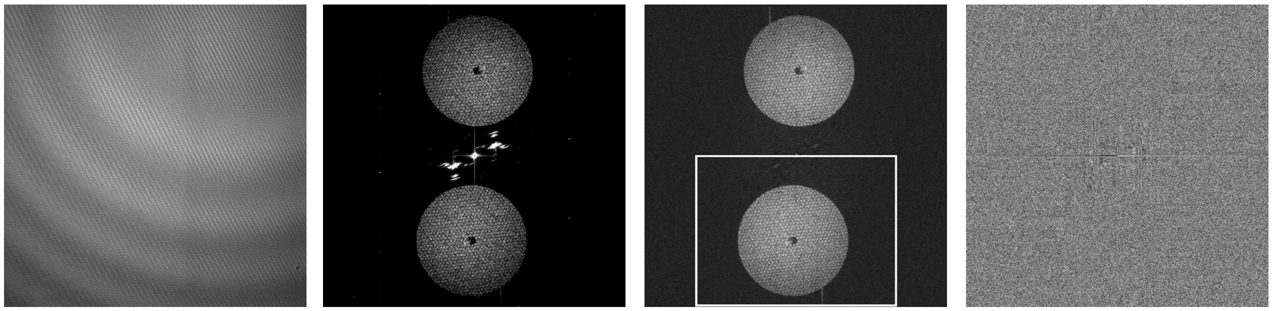

(a) (b) (c) (d)

Figure 3. (a) Digital hologram as recorded by the camera. (b) Modulus of the numerical reconstruction by a single Fourier transform of (a). (c) The result of subtracting the modulus of the reconstructed reference beam to (b); the edges of the aperture, not visible against the dark background, are marked with a white rectangle. (d) The argument of the numerical reconstruction shown in (b).

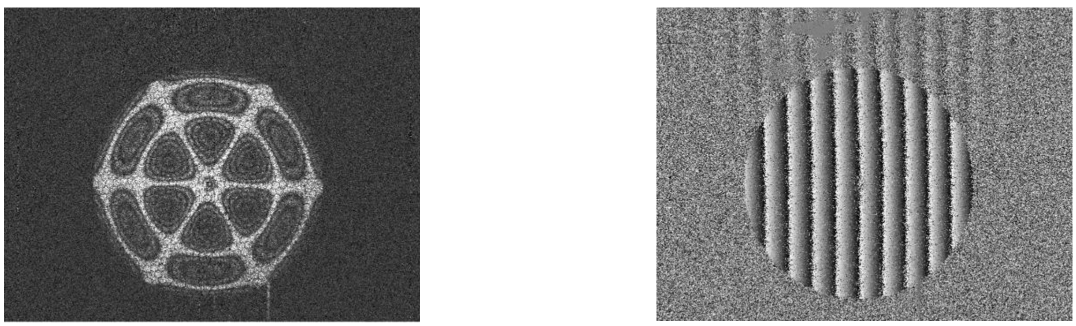

(a) (b)

Figure 4. (a) Time average holographic interferogram of a vibrating disk and (b) double-exposure displacement phase map obtained by tilting the same (non-vibrating) disk around a vertical axis. Both are taken with a zoom lens at a focal length of $f' = 35$mm.

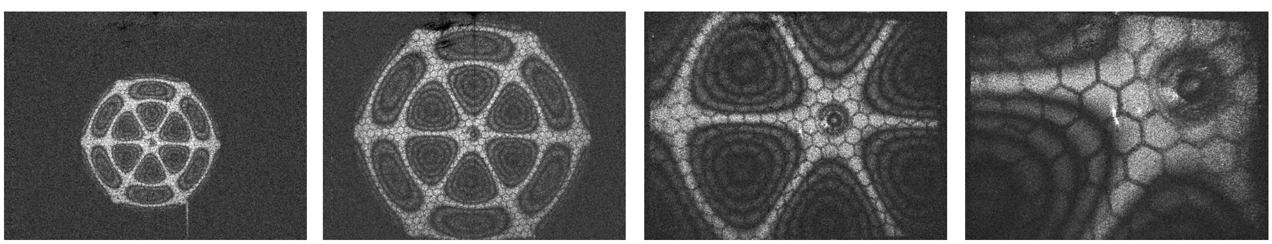

(a) $f' = 28$mm (b) $f' = 50$mm (c) $f' = 90$mm (d) $f' = 210$mm

Figure 5. The same vibration state of figure 4.(a) imaged with two photographic zoom lenses at different focal lengths. A 28–70mm F/3,5–4,5 objective has been used in (a) and (b), and a 70–210mm F/4,0–5,6 objective has been used in (c) and (d).

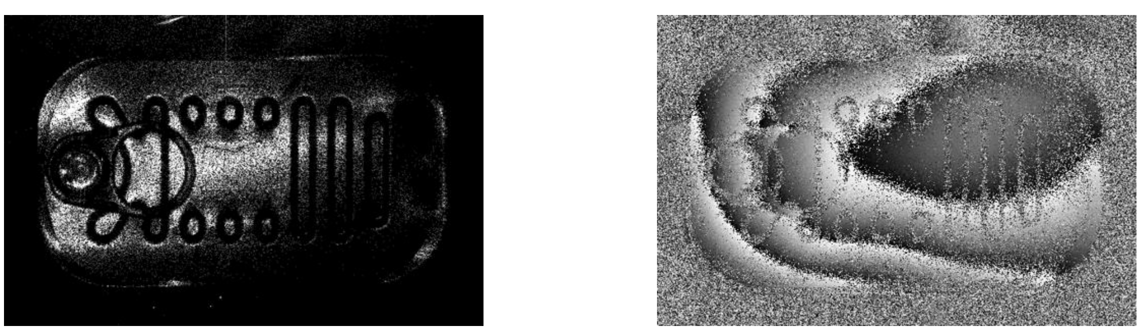

(a) (b)

Figure 6. (a) Amplitude of the reconstruction of an object (an empty tin can for fish) showing specular reflections and (b) contouring phase map obtained by tilting the illumination beam.

Two objects where used to obtain the herein presented sample results: a circular aluminum disc (∅120mm) clamped on its center and coated with retro-reflective tape and an untreated tin can (105mm×60mm) of one of the types used for canned fish. Both objects were placed 1100mm in front of the camera, which is the path equalization distance for our interferometer.

Figure 3 illustrates the recording and reconstruction process. We use a radix-2 FFT algorithm and, consequently, we take just a 1024×1024 pixel region of the sensor. The amplitude separation and reference beam subtraction techniques described in section 2.4 are used to remove the unwanted terms from the amplitude images. Figure 4 demonstrates the operation of the system in the two holographic interferometric modes mentioned in section 2.3. Only the reconstruction of the aperture area is shown in this and in the following images. Figure 5 shows how, with this design, the field of view can be accommodated to cover almost any object or region just by replacing the objective or by changing its focal length as in TV holography, but no adjustments are necessary regardless of the changes of the position of the exit pupil.

One of the advantages of the proposed technique is that it provides reasonable measurements even in presence of localized specular reflections which would saturate TVH systems, because they are spread over the sensor rather than being focused on its surface. An example of this situation is presented in figure 6.

4. CONCLUSIONS

We have presented a novel hybrid digital holographic camera and demonstrated its operation in plain holographic image reconstruction as well as in holographic interferometry operation both in the amplitude and phase modulation modes.

The main advantages of this design are that just one FFT is required to perform the reconstruction of the hologram and, therefore, it is at least twice faster than Fourier-transform evaluation in TVH; since no focused images are formed on the sensor, it is reasonably immune to saturation by localized specular reflections; all the critical elements (sensor, aperture and reference beam) are local, thus allowing to make true remote measurements, are fixed and can be compacted into a ruggedized head to which many different image forming systems can be coupled; the field of view can be accommodated to cover objects of almost any size and placed at any distance by means of the a convenient selection or adjustment of the said optical system, no adjustment is required in the aforementioned critical elements; there is no risk of aliasing due to objects with sizes larger than the field of view or placed out of it.

Its most remarkable drawback is that, as other non imaging holographic methods, it cannot provide images of the object with white light illumination neither good resolution holographic reconstructions in real time when currently available regular computers are used. This makes the process of selecting the field of view and focusing more complicated and time consuming than in TVH.

ACKNOWLEDGMENTS

The authors acknowledge the funding received from the spanish *Ministerio de Educación y Ciencia* and the European Commission (ERDF) within the *Plan Nacional de Investigación Científica, Desarrollo e Innovación Tecnológica* (project number DPI2005-09203-C03-01) as well as from the *Secretaría Xeral de Investigación e Desenvolvemento da Xunta de Galicia* within the *Plan Galego de IDIT* (project number PGIDIT03PXIC30301PN).

REFERENCES

1. H. O. Saldner, N. E. Molin and K. A. Stetson, “Fourier-transform evaluation of phase data in spatially phase-biased TV holograms”, Applied Optics **35**, pp. 332-336, 1996.
2. U. Schnars, and W. Jueptner,. *Digital Holography*, Springer, Berlin 2005.
3. C. Wagner, S. Seebacher, W. Osten and W. Jüptner, “Digital recording and numerical reconstruction of lensless Fourier holograms in optical metrology”, Applied Optics **38**, pp.4812-4820, 1999.
4. S.H. Lee, P.Naulleau, K.A. Goldberg, C.H. Cho, S.T. Jeong and J. Bokor, “Extreme-ultraviolet lensless Fourier-transform holography”, Applied Optics **40**, pp.2655-2661, 2001.
5. R.J. Collier, C.B. Burckhard and L.H. Lin, Optical Holography, p.212, Academic Press, New York, 1971.
6. A. F. Doval, “A systematic approach to TV holography,” Measurement Science & Technology **11**, R1-36, 2000.
7. K. Qian, H. S. Seah and A. K. Asundi, "Algorithm for directly retrieving the phase difference: a generalization", Optical Engineering **40**, pp. 1721-1724, 2003.